Letter | Editors' Suggestion

Bound states in the continuum in multipolar lattices

Sergei Gladyshev, Artem Shalev, Kristina Frizyuk, Konstantin Ladutenko, and Andrey Bogdanov*
School of Physics and Engineering, ITMO University, 191002, St. Petersburg, Russia

(Received 21 February 2022; revised 7 May 2022; accepted 9 May 2022; published 22 June 2022)

We develop a theory of bound states in the continuum (BICs) in multipolar lattices—periodic arrays of resonant multipoles. We predict that BICs are completely robust to changes in the lattice parameters, remaining pinned to specific directions in the k space. The lack of radiation for BICs in such structures is protected by the symmetry of multipoles forming the lattice. We also show that some multipolar lattices can host BICs forming a continuous line in the k space, and such BICs carry zero topological charge. The developed approach sets a direct fundamental relation between the topological charge of BICs and the asymptotic behavior of the Q factor in its vicinity. We believe that our theory is a significant step towards gaining deeper insight into the physics of BICs and the engineering of high-Q states in all-dielectric metasurfaces.

DOI: 10.1103/PhysRevB.105.L241301

Bound states in the continuum (BICs) are nonradiating solutions of the wave equation with the spectrum embedded in the continuum of the propagating modes in the surrounding space [1]. A general wave phenomenon, BICs were first predicted in quantum mechanics [2] but today have found a variety of applications in photonics and acoustics [3–7]. Their strong spatial localization and high-quality (Q) factor provide giant amplification of the external electric field [8] and drastically enhance the light-matter interaction [9–12], nonlinear optical effects [13–16], and the performance of lasers [17–22]. Also, BICs have made it possible to realize a new class of sensing devices due to their highly selective response [23–29].

One of the most used platforms supporting BICs are periodic photonic structures including gratings [30], chains [31], corrugated waveguides [32], metasurfaces [33], and photonic crystal slabs [34]. The periodicity makes radiation possible only through open diffraction channels of which there is a finite number as opposed to a single scatterer where there is an infinite number. To form a BIC one needs to nullify the coupling constants to all of these channels, which can be achieved by either exploiting the symmetry of the structures or by precisely tuning the system's parameters, referred to as *symmetry protected* and *parametric*, respectively [35]. In structures with a subwavelength period, there is only one open diffraction channel that makes the engineering and observation of BICs substantially easier. Symmetry-protected BICs appear in the center of the Brillouin zone (Γ point), while parametric BICs appear out of the Γ point, in the general case. However, due to fine tuning of the geometrical and material parameters of the system, parametric BICs can be moved to the Γ point [36–38].

Dielectric and plasmonic metasurfaces have a strong optical response, usually associated with Mie or plasmonic resonances of meta-atoms [39,40]. Each meta-atom possesses a certain multipolar content that depends on the symmetry of the unit cell and design of the meta-atom [41–43]. However, in the vicinity of the resonances, there usually is only one dominant multipole. Thus, the metasurfaces can be effectively considered as *multipolar lattices*, consisting of particular point multipoles [44–46]. Multipolar lattices extend the concept of single electromagnetic multipoles which proved to be a powerful tool for describing the optical properties of single resonant scatterers and nanoantennas [47–49].

In this Letter, we develop a general theory of BICs in multipolar lattices and show that off-Γ (parametric) BICs, that are usually very sensitive to parameters of the structure, are pinned in the k space to specific directions and they are robust with respect to changes in the resonance frequency of meta-atoms and the lattice period as long as the system remains subwavelength. This theory predicts the existence of BICs forming a continuous line in the k space and sets a direct relation between the topological charge of BIC and the asymptotic behavior of the Q factor in its vicinity.

The main idea of the developed theory is based on the fact that multipoles arranged into a periodic structure radiate as well as a single multipole, but only to the direction of the open diffraction channel [41,42,50,51]. In other words, the polarization of the plane wave radiated by the metasurface is the same as the polarization of the wave radiated by a single multipole along the same direction. The interaction between the multipoles in the lattice affects only the amplitudes of the multipoles but not their radiation pattern. Therefore, the magnitude of the radiated power into the open diffraction channel is proportional to the directivity of the multipole along this direction. Formally, the far field of the subwavelength multipolar lattice can be written as (see Supplemental Material [52])

$$\mathbf{E}(\mathbf{r}) = \frac{S_b}{2\pi k k_z} e^{i\mathbf{k}\mathbf{r}} i^{-\ell} \tilde{D}_s \mathbf{Y}_s\left(\frac{\mathbf{k}}{k}\right). \tag{1}$$

Here, $k = \omega/c$ is the wave number in the surrounding space that is assumed to be air, $\mathbf{k}$ is the total wave vector of the radiated plane wave, and $k_z = \pm\sqrt{k^2 - |\mathbf{k}_b|^2}$, where $\mathbf{k}_b$ is the

*a.bogdanov@metalab.itmo.ru

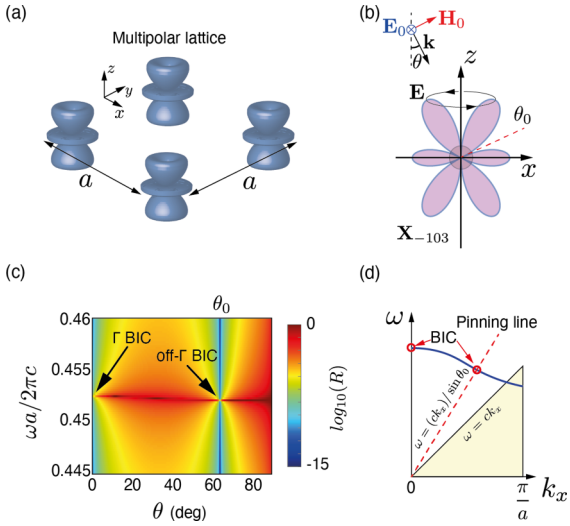

FIG. 1. (a) Concept of the system. Multipolar lattice with a square unit cell and period a containing a single multipole in the unit cell (electric $\mathbf{Z}_{tm\ell}$ or magnetic $\mathbf{X}_{tm\ell}$). (b) The far-field radiation pattern plotted for the magnetic octupole scatterer ($\mathbf{X}_{-103}$) in the xOz plane. The inset shows the polarization of the incident wave. (c) The reflection R from the magnetic octupolar lattice with a square unit cell plotted as a function of dimensionless frequency $\omega a/2\pi c$ and angle of incidence θ for the ratio $a/d = 1.75$ in logarithmic scale. The magnetic octupole $\mathbf{X}_{-103}$ is described by the T matrix of a high-refractive-index sphere neglecting all its scattering channels except for the magnetic octupolar. The permittivity of the sphere is $\varepsilon = 50$ and the diameter is d. (d) Schematic bang diagram for a multipolar lattice demonstrating the pinning of the off-Γ BICs in the k space.

Bloch vector. S_b is the two-dimensional (2D) volume of the first Brillouin zone. $\mathbf{Y}_s = \{\mathbf{X}_s, \mathbf{Z}_s\}$ are the vector spherical functions which describe the far field of each multipole and $\tilde{D}_s$ are the coefficients of the multipolar decomposition. Index s is a set of indices p, m, ℓ, where $l = 0, 1, 2, \ldots$ is the total angular momentum quantum number, and $m = 0, 1, \ldots, \ell$ is the absolute value of the projection of the angular momentum (magnetic quantum number). Index $p = \pm 1$ defines the parity of $\mathbf{Y}_s$ with respect to reflection from the xz plane ($\varphi \to -\varphi$) (see Supplemental Material [52]).

The BICs in a multipolar lattice are formed when the directions of all open diffraction channels coincide with the nodal lines of multipoles forming the lattice [41,42]. For subwavelength lattices, there is only one open diffraction channel, therefore, each nodal line corresponds to a BIC. The directions of the nodal lines and surfaces are completely defined by the multipole $\mathbf{Y}_s(\mathbf{k}/k)$ and they do not depend on the lattice parameters as long as the multipolar composition of the unit cell is assumed to be conserved.

The developed theory is quite general and can be applied to arbitrary multipolar lattices, but to have an illustrative example we consider first a multipolar lattice with a square unit cell of a period a consisting of single magnetic octupoles ($\mathbf{X}_{-103}$) [see Figs. 1(a) and 1(b)]. In numerical simulations, we describe the single multipole by the T matrix of the high-refractive-index sphere with permittivity ε and diameter d, neglecting all its scattering channels except for the one corresponding to the multipole under scrutiny. The numerical code is based on the MULTEM package [56,58] (see Supplemental Material [52]).

Figure 1(c) show the reflection R from the octupolar lattice as a function of frequency ω and angle of incidence θ. The incident wave is assumed to be s polarized [see Fig. 1(b)]. One can see that the octupolar resonance forms a narrow nearly flat band featuring a weak interaction between the multipoles. The resonance becomes infinitely narrow at angles $\theta_0 = 0^\circ$ and 63.4° corresponding to the nodal lines of the octupole manifesting the appearance of the at-Γ and off-Γ BICs. At these angles, the incident wave does not interact with the metasurface and it becomes completely transparent. Therefore, to find the angular position of BICs in the case of an arbitrary multipolar lattice, one needs to solve a system of equations $E_\theta = E_\varphi = 0$, where $\mathbf{E}$ is the far field of the multipole defined by Eq. (1). For our particular case of magnetic octupoles ($\ell = 3, m = 0$), this system is reduced to one equation $P_3'(\cos\theta) = 0$, where P_3 is the Legendre polynomial. The roots of this equation exactly give $\theta_0 = 0^\circ$ and 63.4° predicting the angular position of the BICs.

Figure 1(d) shows schematically how the BICs in a multipolar lattice are formed and pinned to the specific directions of the k space. The blue curve depicts a dispersion band of the metasurface formed by the multipolar resonances. The red dashed curve $\omega = ck_x/\sin\theta_0$ corresponds to the nodal line of the multipole. The BIC is formed exactly at the crossing of the dispersion surface with the nodal lines of the multipole. The dispersion depends on the polarizability of meta-atoms and lattice parameters while the nodal lines do not depend on them at all, which makes off-Γ BICs pinned to the specific directions in k space and robust to the variation of lattice parameters. One should mention that the angular robustness of BICs is ensured by conserving the multipolar composition of the unit cell. The variation of the multipolar compositions results in the migration of BICs within the Brillouin zone.

Figure 2 shows the reflection maps R for multipolar lattices for different a/d ratios. One can see that the variation of the a/d ratio affects only the frequency of the off-Γ BIC but not its angular position. The increase of a/d from 1.5 to 2.25 results in the blueshift of the band due to the enhancement of the interaction between the multipoles. This can lead to the destruction of the BIC if its frequency becomes higher than the diffraction threshold, namely, $\omega a/2\pi c > 1/(1 + \sin\theta_0)$ (see Fig. 2, panel for $a/d = 2.25$). It is worth mentioning that even for frequencies higher than the diffraction threshold the radiative losses along the direction of the nodal line are still forbidden and the radiation occurs through other open diffraction channels. One can say that the lack of radiation along the particular directions is protected by the symmetry of the multipole. A similar effect is observed for symmetry-protected BICs in the dielectric gratings [61].

Higher-order multipoles have a larger number of nodal lines. This results in the appearance of several off-Γ BICs within one band. Figure 3(a) shows the reflection map for the metasurface formed by resonant magnetic multipoles of the fifth order ($\ell = 5; m = 0$). The directivity pattern for such a multipole and its nodal lines corresponding to $\theta_1 = 40.0^\circ$ and $\theta_2 = 73.3^\circ$ are shown in Fig. 3(b). One should mention that as we consider the lattice consisting of multipoles with rotational

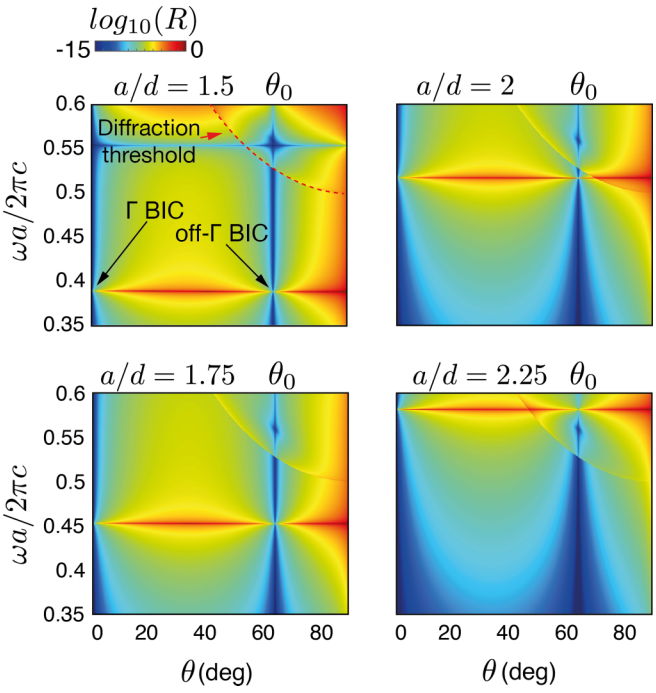

FIG. 2. The reflection R from the magnetic octupolar ($\ell = 3$, $m = 0$) lattice with a square unit cell [see Fig. 1(a)] plotted as a function of dimensionless frequency $\omega a/2\pi c$ and angle of incidence θ for different ratios a/d in logarithmic scale. The period of the structure is a. The magnetic octupole $\mathbf{X}_{-103}$ is described by the T matrix of a high-refractive-index sphere neglecting all its scattering channels except for the magnetic octupolar. The permittivity of the sphere is $\varepsilon = 50$ and the diameter is d. The incident wave is s polarized [see Fig. 1(a)].

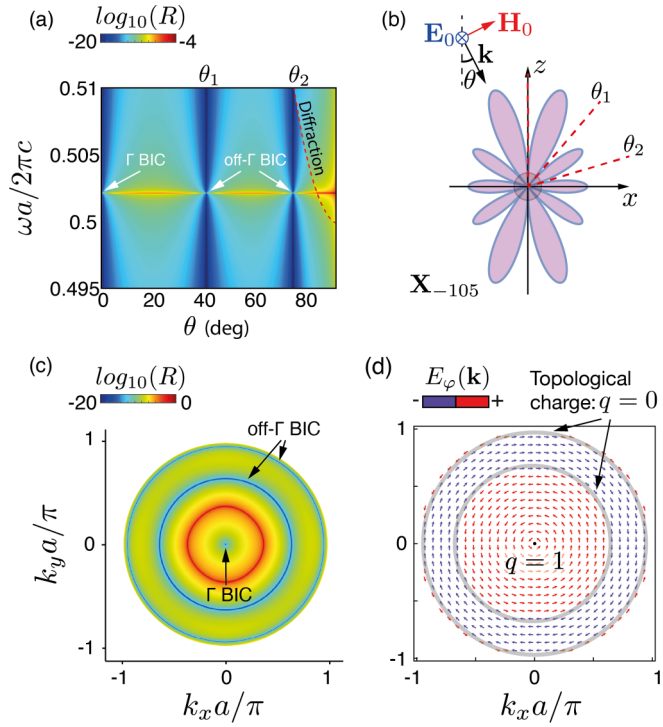

FIG. 3. (a) The reflection R from the magnetic multipolar lattice ($\ell = 5$, $m = 0$) lattice with a square unit cell [see Fig. 1(a)] plotted as a function of dimensionless frequency $\omega a/2\pi c$ and angle of incidence θ for the ratio $a/d = 2$ in logarithmic scale. The period of the structure is a. The magnetic multipole $\mathbf{X}_{-105}$ is described by the T matrix of a high-refractive-index sphere (permittivity $\varepsilon = 220$ and diameter d) neglecting all its scattering channels except the magnetic octupolar. (b) Far-field radiation pattern for $\mathbf{X}_{-105}$. The inset shows the polarization of the incident wave. (c) Reflection map for the same lattice plotted at frequency $\omega a/2\pi c = 0.5$ as a function of the in-plane wave vectors k_x and k_y. (d) Polarization map of the magnetic multipolar band ($\mathbf{X}_{-105}$) in the far field showing the BICs forming a close continuous line in the k space.

symmetry ($m = 0$), the nodal lines are actually nodal surfaces (cones). Thus, the off-Γ BICs form a closed continuous line [38,42,62,63]. As the band is nearly flat the BICs almost form circles in the k space. This can be seen from the reflection map shown in Fig. 3(c).

The BICs in periodic photonic structures can be associated with polarization vortices in the far field which carry a topological charge q that can be calculated as [34]

$$q = \frac{1}{2\pi} \oint_C d\mathbf{k} \cdot \nabla_{\mathbf{k}} \phi(\mathbf{k}), \quad q \in \mathbb{Z}. \tag{2}$$

Here, $\phi(\boldsymbol{k}) = \arg[E_x(\boldsymbol{k}) + iE_y(\boldsymbol{k})]$, E_x and E_y the complex amplitudes of the radiated plane waves, and C is a simple counterclockwise oriented path enclosing the singular point. A reasonable question is, do the BICs forming a continuous line in the k space carry some topological charge? Figure 3(d) shows the polarization map calculated for a multipolar lattice consisting of magnetic multipoles ($\ell = 5$, $m = 0$). The topological charge q carried by an off-Γ BIC forming a closed line in the k space can be defined as the difference between the integrals [Eq. (2)] calculated over closed paths inside and outside the BIC line. Straightforward calculations show that BICs form a line in the case the space of the topological charge $q = 0$. Indeed, as one can see from Fig. 3(d), the polarization vortex inside and outside the BIC line changes only the direction of rotation that does not affect the value of the integral in Eq. (2). This result is in complete accordance with the Poincaré-Hopf theorem that reads that only isolated singularities contribute to the total charge [64].

In theory, BICs can carry an arbitrary high topological charge [34]. Such BICs are quite prospective as they can be more robust to imperfections of the structures and demonstrate higher Q factors [65]. Nevertheless, to date, suggested designs of the photonic crystals and metasurfaces support BICs with a maximal topological charge $|q| = 2$ [12,66]. Quasicrystals due to a high-order rotational symmetry can support high-Q leaky resonances with polarization singularities of a large topological charge [67]. However, the observation of genuine BICs with high topological charges is still a challenge. Still, the multipolar lattices can naturally support them. Indeed, one can see from Eq. (1) that the polarization structure in the vicinity of the Γ point entirely succeeds the far-field polarization structure of the multipole including all polarization singularities [41]. Therefore, to construct a BIC with high topological charge in a multipolar lattice, one needs to take a multipole forming a vortex along the vertical direction with a large topological charge. For example, multipolar

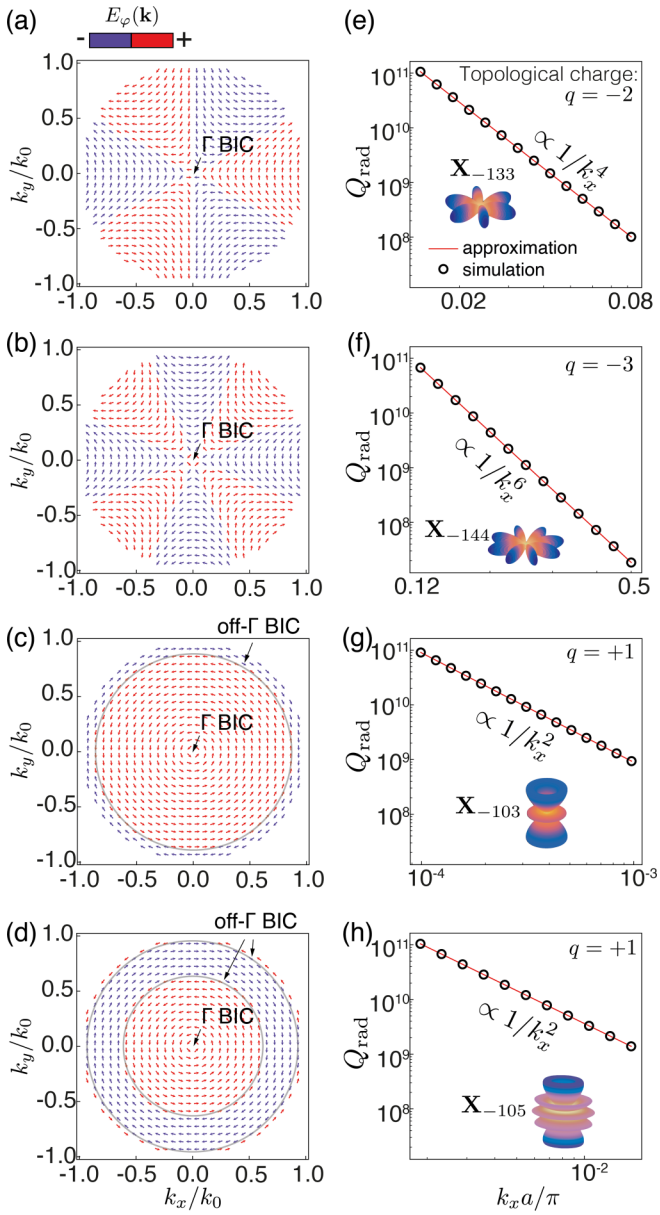

FIG. 4. (a)–(d) Far-field polarization maps of a multipolar lattice composed of various multipoles. (e)–(h) Asymptotic behavior of $Q_{\rm rad}$ in the vicinity of the Γ point plotted for various multipoles (see insets) found numerically and analytically.

lattices consisting of electric or magnetic multipoles with $\ell = m \geqslant 2$ support symmetry-protected BICs with topological charge $q = 1 - \ell$. Figures 4(a) and 4(b) show the polarization maps for the multipolar lattices comprising magnetic multipoles with $\ell = m = 3$ and $\ell = m = 4$, respectively. Applying Eq. (2) to these maps, one can get topological charges $q = -2$ and $q = -3$. Taking higher-order multipoles, one can get BICs with arbitrary high negative topological charges.

The asymptotic behavior of the Q factor in the vicinity of BIC is quite important from a practical point of view as it allows us to predict the robustness of the BIC to the structural imperfections and the dependence of the radiative Q factor on the size of the sample [65,68]. For multipolar lattices, the dependence of the radiative Q factor on the Bloch wave vector $\mathbf{k}_b = (k_x, k_y, 0)$ can be found analytically for the considered multipolar lattices using the following definition, $Q = \omega W_{\rm st}/P_{\rm rad}$, where $W_{\rm st}$ is the energy stored in the unit cell and $P_{\rm rad}$ is the power radiated by the unit cell. Assuming that the multipole is described by the T matrix of a high-refractive-index sphere and all the energy is stored inside the sphere, one can show that the asymptotics of the Q factor for BIC in the vicinity of the Γ point is completely defined by the topological charge of the BIC:

$$Q \sim \frac{1}{|\mathbf{Y}_s(\boldsymbol{k}/k)|^2} \sim \frac{1}{|\mathbf{k}_b|^{2|q|}}. \tag{3}$$

The exact analytical expression is quite cumbersome and we provide it in the Supplemental Material [52]. Figures 4(e)–4(h) show the asymptotics of the Q factor in the vicinity of the Γ point for different multipolar lattices obtained numerically and analytically. The corresponding polarization maps are shown in Figs. 4(a)–4(d).

In conclusion, we analyzed at-Γ and off-Γ BICs in subwavelength multipolar lattices—metasurfaces whose unit cell contains only one resonant multipole. Technically, we describe a single multipole by the T matrix of a high-refractive-index sphere neglecting all its scattering channels except for the one corresponding to the multipole under scrutiny. We predict that the off-Γ BICs in such lattices are pinned to the specific directions in the k space and completely robust against changes of the resonant frequency of the multipole and lattice parameters as long as the structure remains subwavelength. The analyzed BICs are protected by the symmetry of the multipoles. We show that if the multipole has a rotational symmetry with respect the direction normal to the metasurface, the BIC forms a continuous closed line in the k space. The topological charge for such BICs is zero. We reveal that the multipolar lattice can host at-Γ BICs with a high topological charge $|q| > 2$ and set a direct analytical relation between the asymptotics of the Q factor in the vicinity of the BICs and their topological charge. One should necessarily mention that the multipolar lattices containing only one multipole in the unit cell is the only approximation that works well only in the vicinity of the resonance when one multipole dominates over others. A more accurate description requires accounting for other multipoles. We believe that the developed theory and predicted effects are an important step in understanding the physics of bound states in the continuum and their engineering in periodic photonic structures.

The authors thank K. Koshelev, C. Rockstuhl, W. Liu, A. Sadreev, Yu. Kivshar, M. Petrov, and D. Maksimov for useful discussions. The analytical results and simulation were obtained with the support of the Russian Science Foundation Project No. 20-72-10141. S.G., K.F., and A.B. acknowledge the "BASIS" Foundation and the Priority 2030 Federal Academic Leadership Program.

S.G. and A.S. contributed equally to this work.

[1] C. W. Hsu, B. Zhen, A. D. Stone, J. D. Joannopoulos, and M. Soljačić, Bound states in the continuum, Nat. Rev. Mater. **1**, 16048 (2016).

[2] J. von Neumann and E. P. Wigner, Über merkwürdige diskrete eigenwerte, Phys. Z. **30**, 467 (1929).

[3] S. I. Azzam and A. V. Kildishev, Photonic bound states in the continuum: From basics to applications, Adv. Opt. Mater. **9**, 2001469 (2021).

[4] A. F. Sadreev, Interference traps waves in an open system: Bound states in the continuum, Rep. Prog. Phys. **84**, 055901 (2021).

[5] S. Joseph, S. Pandey, S. Sarkar, and J. Joseph, Bound states in the continuum in resonant nanostructures: An overview of engineered materials for tailored applications, Nanophotonics **10**, 4175 (2021).

[6] K. Koshelev, A. Bogdanov, and Y. Kivshar, Meta-optics and bound states in the continuum, Sci. Bull. **64**, 836 (2019).

[7] K. Koshelev, G. Favraud, A. Bogdanov, Y. Kivshar, and A. Fratalocchi, Nonradiating photonics with resonant dielectric nanostructures, Nanophotonics **8**, 725 (2019).

[8] J. W. Yoon, S. H. Song, and R. Magnusson, Critical field enhancement of asymptotic optical bound states in the continuum, Sci. Rep. **5**, 18301 (2015).

[9] M. Qin, S. Xiao, W. Liu, M. Ouyang, T. Yu, T. Wang, and Q. Liao, Strong coupling between excitons and magnetic dipole quasi-bound states in the continuum in WS_2-TiO_2 hybrid metasurfaces, Opt. Express **29**, 18026 (2021).

[10] K. L. Koshelev, S. K. Sychev, Z. F. Sadrieva, A. A. Bogdanov, and I. V. Iorsh, Strong coupling between excitons in transition metal dichalcogenides and optical bound states in the continuum, Phys. Rev. B **98**, 161113(R) (2018).

[11] V. Kravtsov, E. Khestanova, F. A. Benimetskiy, T. Ivanova, A. K. Samusev, I. S. Sinev, D. Pidgayko, A. M. Mozharov, I. S. Mukhin, M. S. Lozhkin *et al.*, Nonlinear polaritons in a monolayer semiconductor coupled to optical bound states in the continuum, Light: Sci. Appl. **9**, 56 (2020).

[12] S. A. Dyakov, M. V. Stepikhova, A. A. Bogdanov, A. V. Novikov, D. V. Yurasov, M. V. Shaleev, Z. F. Krasilnik, S. G. Tikhodeev, and N. A. Gippius, Photonic bound states in the continuum in Si structures with the self-assembled Ge nanoislands, Laser Photonics Rev. **15**, 2000242 (2021).

[13] K. Koshelev, S. Kruk, E. Melik-Gaykazyan, J.-H. Choi, A. Bogdanov, H.-G. Park, and Y. Kivshar, Subwavelength dielectric resonators for nonlinear nanophotonics, Science **367**, 288 (2020).

[14] I. S. Sinev, K. Koshelev, Z. Liu, A. Rudenko, K. Ladutenko, A. Shcherbakov, Z. Sadrieva, M. Baranov, T. Itina, J. Liu *et al.*, Observation of ultrafast self-action effects in quasi-BIC resonant metasurfaces, Nano Lett. **21**, 8848 (2021).

[15] K. Koshelev, Y. Tang, K. Li, D.-Y. Choi, G. Li, and Y. Kivshar, Nonlinear metasurfaces governed by bound states in the continuum, ACS Photonics **6**, 1639 (2019).

[16] G. Zograf, K. Koshelev, A. Zalogina, V. Korolev, R. Hollinger, D.-Y. Choi, M. Zuerch, C. Spielmann, B. Luther-Davies, D. Kartashov *et al.*, High-harmonic generation from resonant dielectric metasurfaces empowered by bound states in the continuum, ACS Photonics **9**, 567 (2022).

[17] V. Mylnikov, S. T. Ha, Z. Pan, V. Valuckas, R. Paniagua-Domínguez, H. V. Demir, and A. I. Kuznetsov, Lasing action in single subwavelength particles supporting supercavity modes, ACS Nano **14**, 7338 (2020).

[18] M. Wu, S. T. Ha, S. Shendre, E. G. Durmusoglu, W.-K. Koh, D. R. Abujetas, J. A. Sánchez-Gil, R. Paniagua-Domínguez, H. V. Demir, and A. I. Kuznetsov, Room-temperature lasing in colloidal nanoplatelets via Mie-resonant bound states in the continuum, Nano Lett. **20**, 6005 (2020).

[19] Y. Wang, Y. Fan, X. Zhang, H. Tang, Q. Song, J. Han, and S. Xiao, Highly controllable etchless perovskite microlasers based on bound states in the continuum, ACS Nano **15**, 7386 (2021).

[20] A. Kodigala, T. Lepetit, Q. Gu, B. Bahari, Y. Fainman, and B. Kanté, Lasing action from photonic bound states in continuum, Nature (London) **541**, 196 (2017).

[21] M.-S. Hwang, H.-C. Lee, K.-H. Kim, K.-Y. Jeong, S.-H. Kwon, K. Koshelev, Y. Kivshar, and H.-G. Park, Ultralow-threshold laser using super-bound states in the continuum, Nat. Commun. **12**, 4135 (2021).

[22] J.-H. Yang, Z.-T. Huang, D. N. Maksimov, P. S. Pankin, I. V. Timofeev, K.-B. Hong, H. Li, J.-W. Chen, C.-Y. Hsu, Y.-Y. Liu *et al.*, Low-threshold bound state in the continuum lasers in hybrid lattice resonance metasurfaces, Laser Photonics Rev. **15**, 2100118 (2021).

[23] K.-H. Kim and I.-P. Kim, Quasi-bound states in the continuum with high Q-factors in metasurfaces of lower-index dielectrics supported by metallic substrates, RSC Adv. **12**, 1961 (2022).

[24] Z. Tagay and C. Valagiannopoulos, Highly selective transmission and absorption from metasurfaces of periodically corrugated cylindrical particles, Phys. Rev. B **98**, 115306 (2018).

[25] T. C. Tan, Y. K. Srivastava, R. T. Ako, W. Wang, M. Bhaskaran, S. Sriram, I. Al-Naib, E. Plum, and R. Singh, Active control of nanodielectric-induced THz quasi-BIC in flexible metasurfaces: A platform for modulation and sensing, Adv. Mater. **33**, 2100836 (2021).

[26] S. Romano, G. Zito, S. Torino, G. Calafiore, E. Penzo, G. Coppola, S. Cabrini, I. Rendina, and V. Mocella, Label-free sensing of ultralow-weight molecules with all-dielectric metasurfaces supporting bound states in the continuum, Photonics Res. **6**, 726 (2018).

[27] J. Wang, J. Kühne, T. Karamanos, C. Rockstuhl, S. A. Maier, and A. Tittl, All-dielectric crescent metasurface sensor driven by bound states in the continuum, Adv. Funct. Mater. **31**, 2104652 (2021).

[28] A. Tittl, A. Leitis, M. Liu, F. Yesilkoy, D.-Y. Choi, D. N. Neshev, Y. S. Kivshar, and H. Altug, Imaging-based molecular barcoding with pixelated dielectric metasurfaces, Science **360**, 1105 (2018).

[29] D. N. Maksimov, V. S. Gerasimov, S. Romano, and S. P. Polyutov, Refractive index sensing with optical bound states in the continuum, Opt. Express **28**, 38907 (2020).

[30] E. Bulgakov, D. Maksimov, P. Semina, and S. Skorobogatov, Propagating bound states in the continuum in dielectric gratings, J. Opt. Soc. Am. B **35**, 1218 (2018).

[31] M. S. Sidorenko, O. N. Sergaeva, Z. F. Sadrieva, C. Roques-Carmes, P. S. Muraev, D. N. Maksimov, and A. A. Bogdanov, Observation of an Accidental Bound State in the Continuum in a Chain of Dielectric Disks, Phys. Rev. Applied **15**, 034041 (2021).

[32] H. Hemmati and R. Magnusson, Resonant dual-grating metamembranes supporting spectrally narrow bound states in the continuum, Adv. Opt. Mater. **7**, 1900754 (2019).

[33] L. Cong and R. Singh, Symmetry-protected dual bound states in the continuum in metamaterials, Adv. Opt. Mater. **7**, 1900383 (2019).

[34] B. Zhen, C. W. Hsu, L. Lu, A. D. Stone, and M. Soljačić, Topological Nature of Optical Bound States in the Continuum, Phys. Rev. Lett. **113**, 257401 (2014).

[35] C. W. Hsu, B. Zhen, J. Lee, S.-L. Chua, S. G. Johnson, J. D. Joannopoulos, and M. Soljačić, Observation of trapped light within the radiation continuum, Nature (London) **499**, 188 (2013).

[36] E. N. Bulgakov and D. N. Maksimov, Bound states in the continuum and polarization singularities in periodic arrays of dielectric rods, Phys. Rev. A **96**, 063833 (2017).

[37] S. Xiao, M. Qin, J. Duan, F. Wu, and T. Liu, Polarization-controlled dynamically switchable high-harmonic generation from all-dielectric metasurfaces governed by dual bound states in the continuum, Phys. Rev. B **105**, 195440 (2022).

[38] A. S. Kostyukov, V. S. Gerasimov, A. E. Ershov, and E. N. Bulgakov, Ring of bound states in the continuum in the reciprocal space of a monolayer of high-contrast dielectric spheres, Phys. Rev. B **105**, 075404 (2022).

[39] C. Cherqui, M. R. Bourgeois, D. Wang, and G. C. Schatz, Plasmonic surface lattice resonances: Theory and computation, Acc. Chem. Res. **52**, 2548 (2019).

[40] P. Tonkaev and Y. Kivshar, High-Q dielectric Mie-resonant nanostructures (brief review), JETP Lett. **112**, 615 (2020).

[41] W. Chen, Y. Chen, and W. Liu, Singularities and Poincaré Indices of Electromagnetic Multipoles, Phys. Rev. Lett. **122**, 153907 (2019).

[42] Z. Sadrieva, K. Frizyuk, M. Petrov, Y. Kivshar, and A. Bogdanov, Multipolar origin of bound states in the continuum, Phys. Rev. B **100**, 115303 (2019).

[43] S. Gladyshev, K. Frizyuk, and A. Bogdanov, Symmetry analysis and multipole classification of eigenmodes in electromagnetic resonators for engineering their optical properties, Phys. Rev. B **102**, 075103 (2020).

[44] A. S. Kostyukov, I. L. Rasskazov, V. S. Gerasimov, S. P. Polyutov, S. V. Karpov, and A. E. Ershov, Multipolar lattice resonances in plasmonic finite-size metasurfaces, in *Photonics*, Vol. 8 (Multidisciplinary Digital Publishing Institute, Basel, 2021), p. 109.

[45] D. R. Abujetas, J. Olmos-Trigo, J. J. Sáenz, and J. A. Sánchez-Gil, Coupled electric and magnetic dipole formulation for planar arrays of particles: Resonances and bound states in the continuum for all-dielectric metasurfaces, Phys. Rev. B **102**, 125411 (2020).

[46] D. R. Abujetas, J. Olmos-Trigo, and J. A. Sánchez-Gil, Tailoring accidental double bound states in the continuum in all-dielectric metasurfaces, Adv. Opt. Mater., 2200301 (2022).

[47] R. Alaee, C. Rockstuhl, and I. Fernandez-Corbaton, Exact multipolar decompositions with applications in nanophotonics, Adv. Opt. Mater. **7**, 1800783 (2019).

[48] X. G. Santiago, M. Hammerschmidt, S. Burger, C. Rockstuhl, I. Fernandez-Corbaton, and L. Zschiedrich, Decomposition of scattered electromagnetic fields into vector spherical wave functions on surfaces with general shapes, Phys. Rev. B **99**, 045406 (2019).

[49] A. E. Krasnok, A. E. Miroshnichenko, P. A. Belov, and Y. S. Kivshar, All-dielectric optical nanoantennas, Opt. Express **20**, 20599 (2012).

[50] R. Paniagua-Domínguez, Y. F. Yu, A. E. Miroshnichenko, L. A. Krivitsky, Y. H. Fu, V. Valuckas, L. Gonzaga, Y. T. Toh, A. Y. S. Kay, B. Luk'yanchuk *et al.*, Generalized Brewster effect in dielectric metasurfaces, Nat. Commun. **7**, 10362 (2016).

[51] K. Ohtaka, Energy band of photons and low-energy photon diffraction, Phys. Rev. B **19**, 5057 (1979).

[52] See Supplemental Material at http://link.aps.org/supplemental/10.1103/PhysRevB.105.L241301 for additional information and detailed derivations of the equations from the main text, which includes Refs. [53–60].

[53] J. A. Stratton, *Electromagnetic Theory* (McGraw-Hill, New York, 1941).

[54] C. F. Bohren and D. R. Huffman, *Absorption and Scattering of Light by Small Particles* (Wiley, New York, 1983).

[55] N. Stefanou, V. Yannopapas, and A. Modinos, Heterostructures of photonic crystals: Frequency bands and transmission coefficients, Comput. Phys. Commun. **113**, 49 (1998).

[56] V. Y. N. Stefanou and A. Modinos, MULTEM (1998), http://cpc.cs.qub.ac.uk/summaries/ADIM_v2_0.html.

[57] S. G. Johnson, Faddeeva package, http://ab-initio.mit.edu/wiki/index.php/Faddeeva_Package.

[58] K. Ladutenko and A. Shalev, MULTEM (modified version) (2021), https://github.com/wave-scattering/amos-try.

[59] A. A. Bogdanov, K. L. Koshelev, P. V. Kapitanova, M. V. Rybin, S. A. Gladyshev, Z. F. Sadrieva, K. B. Samusev, Y. S. Kivshar, and M. F. Limonov, Bound states in the continuum and Fano resonances in the strong mode coupling regime, Adv. Photonics **1**, 016001 (2019).

[60] K. Ladutenko, Mie calculator, https://physics.itmo.ru/en/mie#/spectrum.

[61] Z. F. Sadrieva, I. S. Sinev, K. L. Koshelev, A. Samusev, I. V. Iorsh, O. Takayama, R. Malureanu, A. A. Bogdanov, and A. V. Lavrinenko, Transition from optical bound states in the continuum to leaky resonances: Role of substrate and roughness, ACS Photonics **4**, 723 (2017).

[62] E. N. Bulgakov and D. N. Maksimov, Bound states in the continuum and Fano resonances in the Dirac cone spectrum, J. Opt. Soc. Am. B **36**, 2221 (2019).

[63] A. Cerjan, C. W. Hsu, and M. C. Rechtsman, Bound States in the Continuum through Environmental Design, Phys. Rev. Lett. **123**, 023902 (2019).

[64] J. Milnor and D. W. Weaver, *Topology from the Differentiable Viewpoint*, Vol. 21 (Princeton University Press, Princeton, NJ, 1997).

[65] J. Jin, X. Yin, L. Ni, M. Soljačić, B. Zhen, and C. Peng, Topologically enabled ultrahigh-Q guided resonances

robust to out-of-plane scattering, Nature (London) **574**, 501 (2019).

[66] T. Yoda and M. Notomi, Generation and Annihilation of Topologically Protected Bound States in the Continuum and Circularly Polarized States by Symmetry Breaking, Phys. Rev. Lett. **125**, 053902 (2020).

[67] Z. Che, Y. Zhang, W. Liu, M. Zhao, J. Wang, W. Zhang, F. Guan, X. Liu, W. Liu, L. Shi, and J. Zi, Polarization Singularities of Photonic Quasicrystals in Momentum Space, Phys. Rev. Lett. **127**, 043901 (2021).

[68] Z. F. Sadrieva, M. A. Belyakov, M. A. Balezin, P. V. Kapitanova, E. A. Nenasheva, A. F. Sadreev, and A. A. Bogdanov, Experimental observation of a symmetry-protected bound state in the continuum in a chain of dielectric disks, Phys. Rev. A **99**, 053804 (2019).